Interplay of plasmonic and charge transfer effects for ultrasensitive Ag–WO₃/TiO₂ photonic crystal SERS sensors

Maria-Athina Apostolaki,[a] Elias Sakellis,[a,b] Spiros Gardelis [a] and Vlassis Likodimos *[a]

[a]*Section of Condensed Matter Physics, Department of Physics, National and Kapodistrian University of Athens, University Campus, 15784 Athens, Greece*
[b]*Institute of Nanoscience and Nanotechnology, National Center for Scientific Research "Demokritos", Agia Paraskevi, 15341 Athens, Greece*
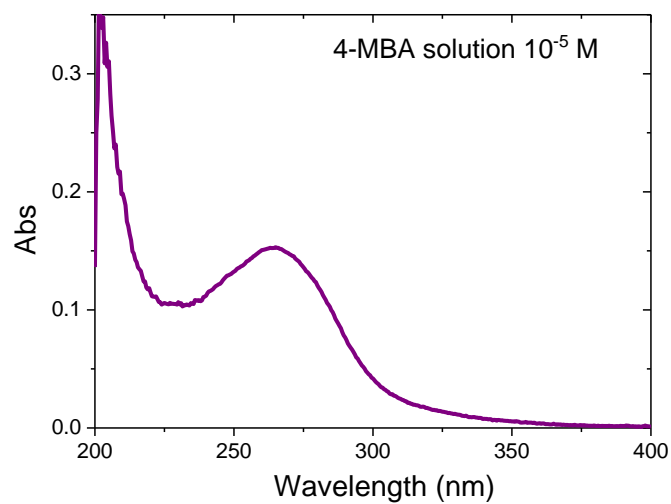
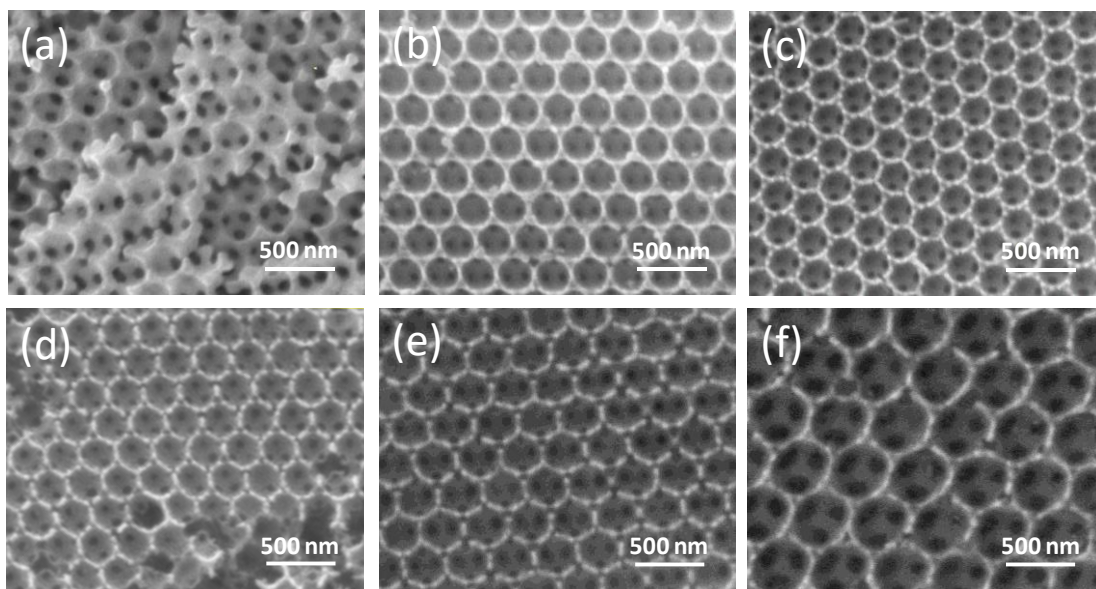**Fig. S1** Absorbance spectra of 4-MBA 10^{-5} M ethanol solution.

Fig. S2 SEM images for (a) PC300 WO_3, (b) PC300 4:1, (c) PC300 1:2, (d) PC300 TiO_2, (e) PC340 TiO_2 and (f) PC406 TiO_2 films.
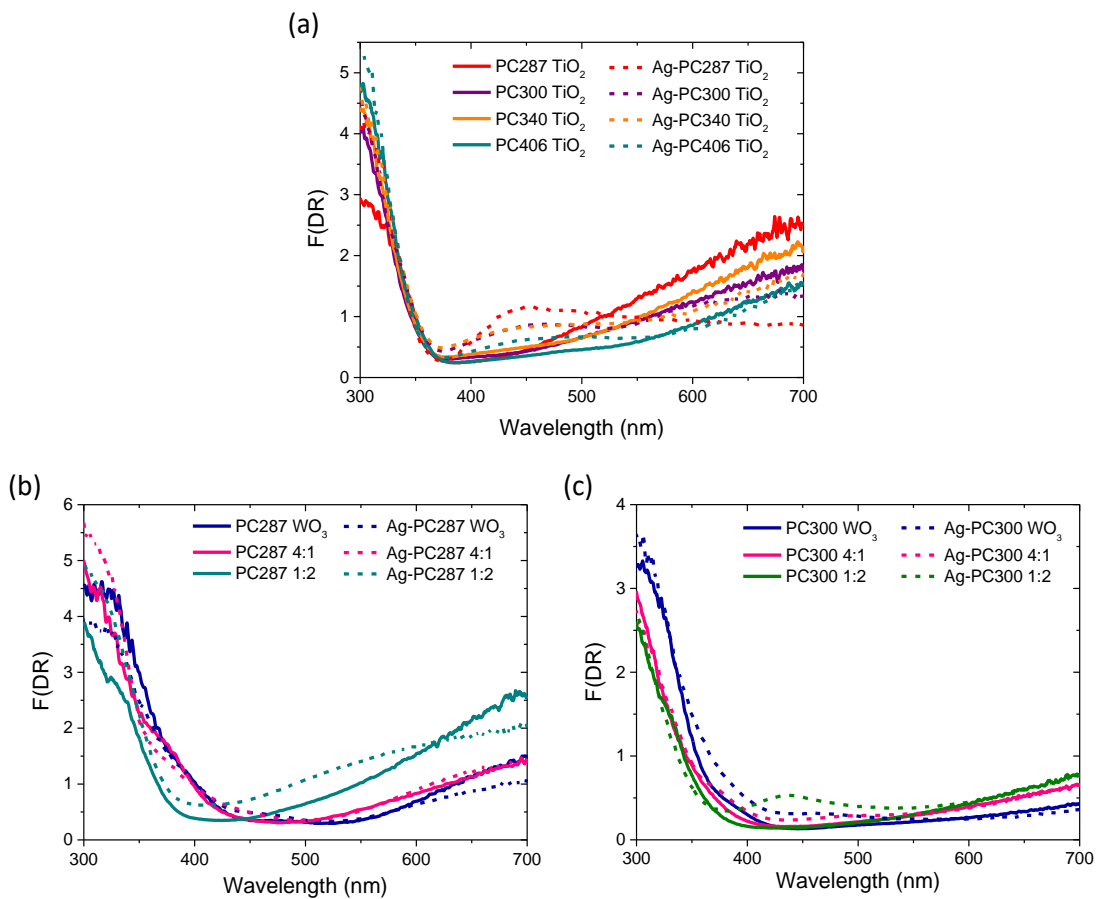
Fig. S3 Kubelka-Munk plots for the (a) TiO_2 PC films and the single WO_3 and composite WO_3/TiO_2 (b) PC287 and (c) PC300 films before and after Ag-deposition.
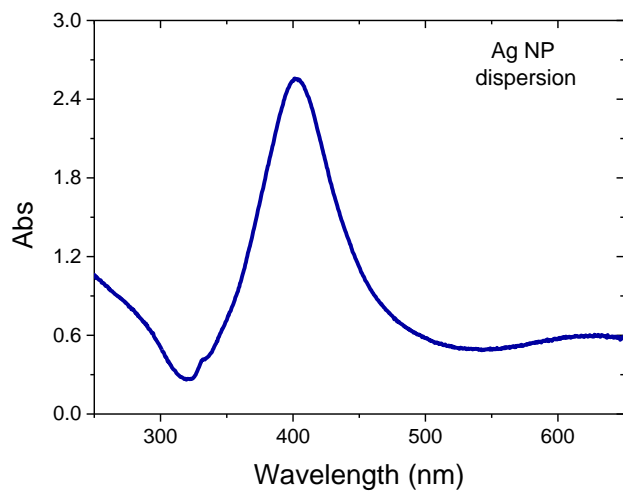

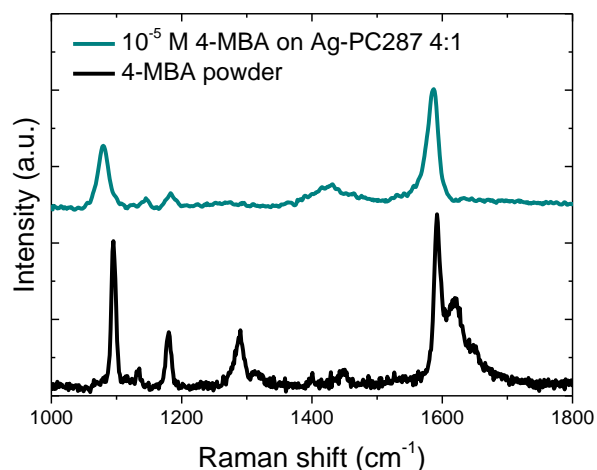**Fig. S4** Absorbance spectra of Ag NPs dispersion.

Fig. S5 Raman spectra of 4-MBA powder and 10^{-5} M solution on the Ag-PC287 4:1 substrate at 532 nm.

The average SERS enhancement factor (EF) was estimated using the most intense 4–MBA vibration at 1585 cm^{-1} for the best performing Ag–PC287 4:1 substrate according to the relation[1]:

$$\text{EF} = \frac{I_{SERS} / N_{SERS}}{I_{bulk} / N_{bulk}}$$

where I_{SERS} and I_{bulk} are the Raman intensities of the selected 4-MBA Raman band for the PC substrate and the reference solid 4-MBA powder. N_{SERS} is the number of adsorbed 4-MBA molecules within the laser spot area (A_{spot}) during SERS measurements, while N_{bulk} is the number of analyte molecules in the scattering volume of the powder sample, approximated as a cylinder of area A_{spot} and effective height h, which corresponds to the confocal depth of the focused laser beam of about 30 μm for a ×40 (NA=0.65) dry objective at 532 nm.[2,3] Thus, N_{bulk} is given by

$$N_{bulk} = \frac{m}{M} N_A = \frac{\rho A_{spot} h N_A}{M},$$

where m is the mass of the 4-MBA molecules within the scattering volume in the normal Raman measurement, $\rho = 1.5$ g/cm^3 is the density and $M = 154.18$ g/mol the molar mass of 4-MBA and N_A is the Avogadro's number. N_{SERS} is given by

$$N_{SERS} = \frac{C V N_A A_{spot}}{A_{film}}$$

where C is the concentration [M] of the 4-MBA solution, V is the volume of the drop casted on the SERS substrate, and A_{film} is the area of the SERS substrates. The EF is accordingly is reduced to

$$\text{EF} = \frac{I_{SERS}}{I_{bulk}} \frac{N_{bulk}}{N_{SERS}} = \frac{I_{SERS}}{I_{bulk}} \frac{\rho A_{film} h}{C V M}$$
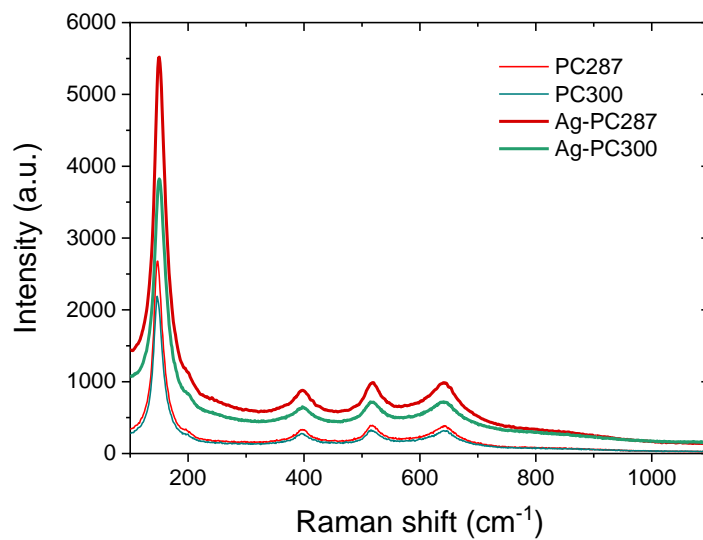
Fig. S6 Comparative Raman spectra of the TiO_2 PC287 and PC300 films before (thin lines) and after Ag deposition (thick lines) at 532 nm.
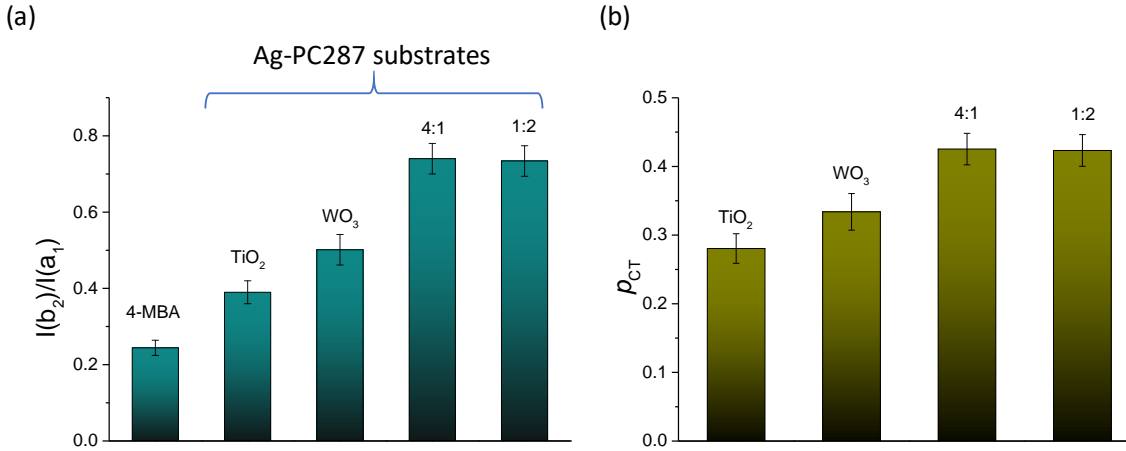
Fig. S7 (a) The intensity ratio of the non-totally (1140 cm^{-1}, b$_2$) to the totally (1182 cm^{-1}, a$_1$) symmetric mode of 4-MBA (10^{-4} M) for the Ag-PC287 substrates. (b) The variation of the corresponding degree of charge transfer given by p_{CT} for the Ag-PC287 substrates.

According to Lombardi and Birke[4], the relative contribution of charge transfer (CT) to the intensity of a specific Raman mode k is defined by the ratio p_{CT} :

$$p_{CT}(k) = \frac{I^k(CT) - I^k(SPR)}{I^k(CT) + I^0(SPR)}$$

where k is the index for the vibrational mode, whose SERS intensity $I^k(CT)$ is enhanced by CT resonance. The calculation of p_{CT} is based on the selection of two reference Raman bands. For a totally symmetric mode, its intensity, defined as $I^0(SPR)$, arises solely from the contribution of surface plasmon resonance (SPR). In the case of a non-totally symmetric k mode, its intensity is mainly determined from the CT contribution $I^k(CT)$, whereas the SPR contribution is very small and thus $I^k(SPR)$ can be neglected. In the present case, p_{CT} was calculated using the intensities of the non-totally (1140 cm^{-1}, b$_2$) and the totally (1182 cm^{-1}, a$_1$) symmetric vibrational modes of 4-MBA as $I^k(CT)$ and $I^0(SPR)$, respectively.[5]
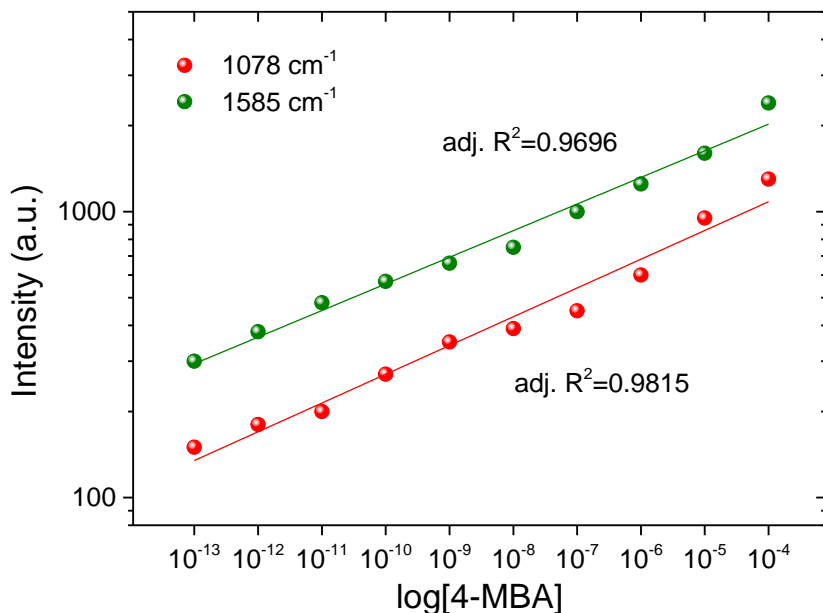
Fig. S8 Raman intensity of the 1079 and 1585 cm^{-1} modes as a function of the 4-MBA concentration. Solid lines show the best fit curves with the corresponding adjusted R^2 values.
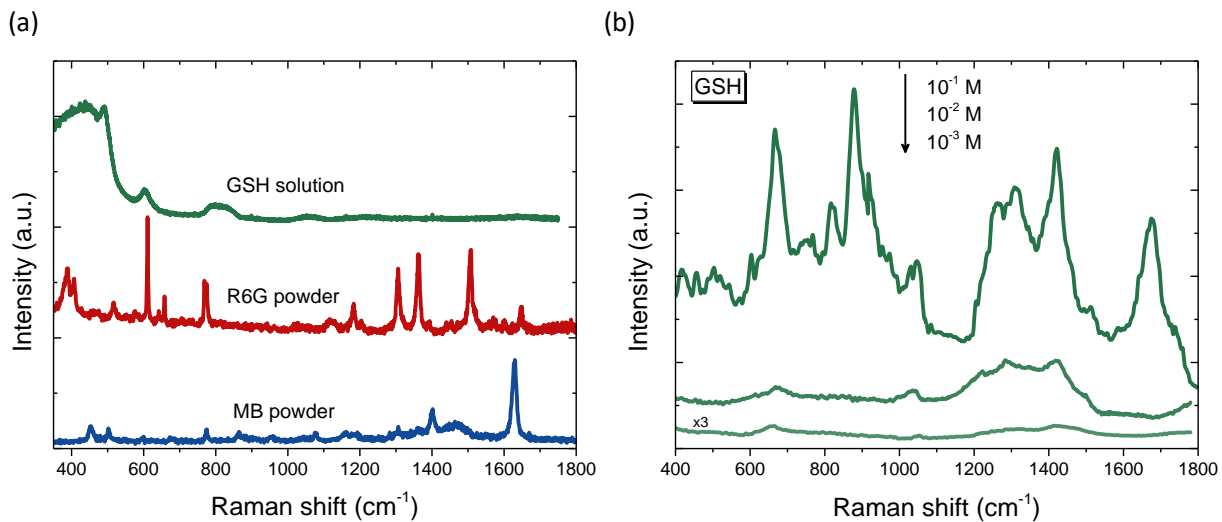

Fig. S9 (a) Raman spectra of 0.1 M GSH aqueous solution, R6G and MB powder samples. (b) Raman spectra of GSH solutions of variable concentrations on the Ag-PC287 4:1 substrate. The excitation wavelength for R6G and MB powder samples was 532 nm, while for GSH solutions its was 785 nm.

Table S1 Structural and optical properties of Ag–WO$_3$/TiO$_2$ PC substrates.

Substrate	D[1] (nm)	Variation[2] %	λ_{exp} (15°)[3] (nm)	n_{eff}	1–f	λ (0°)[4] (nm)
Ag–PC287 WO$_3$	235(5)	82(2)	495	1.32(3)	0.23(2)	504
Ag–PC287 4:1	220(5)	77(2)	475	1.33(3)	0.22(1)	485
Ag–PC287 1:2	190(5)	66(2)	418	1.37(3)	0.20(2)	426
Ag–PC287 TiO$_2$	170(5)	59(2)	368	1.42(4)	0.19(2)	375
Ag–PC300 WO$_3$	245(5)	82(2)	515	1.31(3)	0.23(2)	525
Ag–PC300 4:1	225(5)	75(2)	490	1.35(3)	0.23(1)	498
Ag–PC300 1:2	195(5)	65(2)	434	1.39(3)	0.21(1)	442
Ag–PC300 TiO$_2$	175(5)	58(2)	390	1.39(4)	0.17(2)	397
Ag–PC340 TiO$_2$	215(5)	62(2)	474	1.37(3)	0.16(2)	483
Ag–PC406 TiO$_2$	250(5)	62(2)	492	1.24(3)	0.10(1)	503

[1] D: macropore diameter of the Ag–WO$_3$/TiO$_2$ photonic crystal films determined by SEM.

[2] Macropore variation: D/D$_{sphere}$.

[3] λ_{exp} (15°): PBG position determined from the 15° incidence specular spectra.

[4] λ (0°): PBG position calculated from modified Bragg law at θ=0°.

The photonic band gap (PBG) positions were estimated by modified Bragg's law for first-order diffraction from the (111) fcc planes[6]:

$$\lambda = 2d_{111}\sqrt{n_{eff}^2 - \sin^2\theta}$$

where λ is the PGB wavelength, $d_{111} = \sqrt{2/3}D$ is the spacing between (111) planes, D is the macropore diameter and θ is the angle between the incident beam and the plane normal. The effective refractive index n_{eff} is calculated as $n_{eff}^2 = n_{void}^2 f + n_{MO}^2(1-f)$, where the refractive indices n_{void} and n_{MO} correspond to the void spheres and metal oxides that occupy the inverse opal skeleton for $n_{WO_3} = 2.03$, $n_{TiO_2} = 2.55$ and $n_{air} = 1$, while f is the void filling fraction with the value of 0.74 for the ideal fcc lattice. Stop band positions were estimated for normal incidence ($\theta = 0°$) using the obtained filling fractions.

References

1   E. C. Le Ru, E. Blackie, M. Meyer and P. G. Etchegoin, *J. Phys. Chem. C*, 2007, **111**, 13794–13803.
2   W. B. Cai, B. Ren, X. Q. Li, C. X. She, F. M. Liu, X. W. Cai and Z. Q. Tian, *Surf. Sci.*, 1998, **406**, 9-22.
3   P. Tomba, M. P. Miguel and C. J. Perez, *J. Raman Spectrosc.*, 2011, **42**, 1330–1334.
4   J. R. Lombardi and R. L. Birke, *J. Phys. Chem. C*, 2008, **112**, 5605–5617.
5   X. Jiang, D. Yina, M. Yang, J. Du, W. Wang, L. Zhang, L. Yang, X. Han and B. Zhao, *Appl. Surf. Sci.*, 2019, **487**, 938–944.
6   V. Likodimos, *Appl. Catal. B Environ.*, 2018, **230**, 269–303.